ChemComm

Check for updates

Direct observation of an ionic cobalt complex electron mediator *via operando* X-ray absorption spectroscopy in photocatalytic Z-scheme CO_2 reduction with $(CuGa)_{0.3}Zn_{1.4}S_2$ and $BiVO_4$

Tomiko M. Suzuki, [ID] *[a] Takamasa Nonaka, [ID] [a] Takeshi Uyama, [ID] [a]
Naonari Sakamoto, [ID] [a] Keita Sekizawa, [ID] [a] Yuichi Yamaguchi, [ID] [bc] Akihiko Kudo *[bc]
and Takeshi Morikawa [ID] *[a]

Real-time Co(II)/Co(III) redox state transitions of cobalt complex electron mediators during aqueous Z-scheme CO_2 reduction with oxide and sulfide photocatalysts were directly observed by *operando* X-ray absorption spectroscopy. This approach provides a general framework for advancing mechanistic understanding of ionic redox mediator-driven artificial photosynthesis.

Photocatalytic CO_2 reduction under ambient temperature and pressure using solar energy and water as raw materials---commonly referred to as artificial photosynthesis—is considered a key technology for achieving a carbon-neutral society in the future. To utilize visible light and water, a Z-scheme mechanism (a two-step photoexcitation) employing two different semiconductor photocatalysts for CO_2 reduction and H_2O oxidation is required, similar to natural photosynthesis. This system requires an electron transfer pathway to connect the two half-reactions, categorized into (i) ionic solution-mediated Z-schemes and (ii) heterogeneous Z-schemes employing solid electron mediators or direct coupling of semiconductor photocatalysts.[1]

Ionic solution-mediated Z-scheme systems (type i) have been developed with a variety of redox mediators and photocatalyst combinations, where the mediator plays a crucial role in determining the efficiency and selectivity of CO_2 reduction. Among these, systems employing water-soluble ionic cobalt(II) complex redox mediators with ligands such as terpyridine (tpy) or bipyridine (bpy) have achieved highly selective CO_2 reduction.[2,3] By changing the ligand structure, the redox potential of the Co(II)/Co(III) couple can be precisely tuned to lie between the conduction band minimum of the water oxidation photocatalyst and the valence band maximum of the CO_2 reduction photocatalyst, thereby promoting more efficient electron transfer.

We demonstrated a Z-scheme CO_2 reduction system comprising a divalent $[Co(4,4'\text{-dimethyl-2,2'-bipyridine})_3]^{2+}$ (hereafter described as [Co(II)-dmbpy]) complex as the redox mediator, $BiVO_4$ as the water oxidation photocatalyst, and $(CuGa)_{0.3}Zn_{1.4}S_2$ (CGZS) as the CO_2 reduction photocatalyst (Fig. 1(a)). The photocatalytic system achieved high CO selectivity ($>95\%$) relative to H_2 and stable operation in an aqueous CO_2-flow reactor for over 50 h of visible-light irradiation.[3] Time-dependent evolution of O_2, which is the oxidation product of water, started after an induction period of
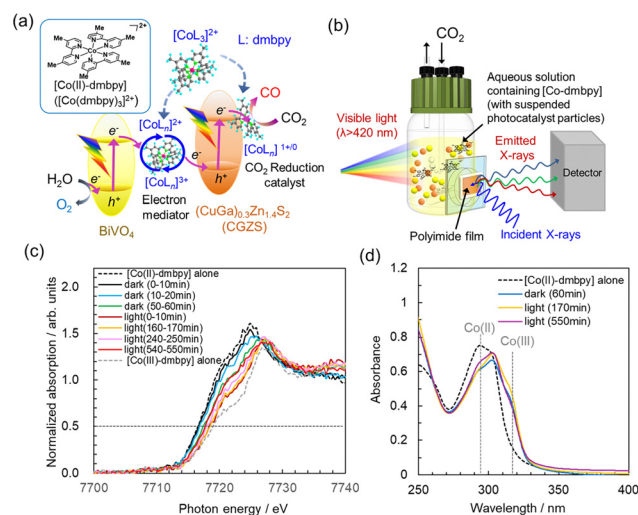

Fig. 1 (a) Z-Scheme photocatalytic CO_2 reduction using particulate $(CuGa)_{0.3}Zn_{1.4}S_2$ (CGZS), $BiVO_4$, and a water-soluble cobalt(II) complex [Co(II)-dmbpy]. About 98% of [Co-dmbpy] functions as a redox electron mediator, while 2% functions as a CO_2 reduction catalyst over CGZS. (b) Schematic illustration of *operando* XAS measurement setup for Z-scheme photocatalytic CO_2 reduction under CO_2 flow. (c) Co K-edge *operando* XANES spectra and (d) *ex situ* UV-Vis spectra of Z-scheme CO_2 reduction, after 60 min in the dark (before (dark)) and continuous visible light irradiation. Times in brackets indicate retention time in the dark or under light irradiation. For UV-Vis measurements, the reaction solution was sampled, the photocatalyst was filtered and diluted 12-fold with a CO_2-saturated 0.01 M $NaHCO_3$ solution.

[a] Toyota Central R&D Labs. Inc., 41-1, Yokomichi, Nagakute, Aichi 480-1192, Japan.
E-mail: tomiko@mosk.tytlabs.co.jp, morikawa@mosk.tytlabs.co.jp

[b] Department of Applied Chemistry, Faculty of Science, Tokyo University of Science,
1-Kagurazaka, Shinjuku-ku, Tokyo 162-8601, Japan. E-mail: a-kudo@rs.tus.ac.jp

[c] Carbon Value Research Center, Research Institute for Science & Technology, Tokyo
University of Science, 2641 Yamazaki, Noda-shi, Chiba 278-8510, Japan

approximately 6 h, although not stoichiometrically sufficient. 98% of [Co(II)-dmbpy] acts as a redox shuttle mediator between CGZS and BiVO$_4$, while 2% serves as a CO$_2$-to-CO conversion cocatalyst on CGZS as a structurally transformed Co(I)[4] which has little effect on the Co(II)/Co(III) mediator cycle.[3]

To further elucidate the Z-scheme mechanism in this metal-complex/semiconductor hybrid photocatalytic system, dynamic monitoring of the redox-state change of the Co complex redox mediator, which facilitates electron transfer between the two semiconductor photocatalysts, is essential. The state of Co species in solution has been investigated using *ex situ* UV-Vis spectroscopy, but it requires sampling of the reaction solution, removal of the photocatalyst, and more than ten-fold dilution,[4] making it impossible to obtain real-time information. Thus the function and behavior of [Co(II)-dmbpy] as an electron transfer mediator remain insufficiently understood.

Here, *operando* X-ray absorption spectroscopy (XAS) was applied for the direct measurement and understanding the behavior of the major portion of [Co(II)-dmbpy] complex as the mediator, which continuously shuttles electrons from BiVO$_4$ to CGZS photocatalysts. Recently, there has been growing interest in *operando* XAS to study dynamic changes in cocatalysts supported on semiconductor surfaces during photocatalytic and photoelectrochemical reactions.[5] Studies have reported changes in the oxidation and reduction state of Pt and Co cocatalysts supported on UV-responsive semiconductors like TiO$_2$ or SrTiO$_3$, providing valuable insights into their catalytic roles.[6] However, no studies have been reported that apply this technique to redox-shuttle electron mediators in aqueous Z-scheme photocatalytic systems. Previously, we conducted *operando* XAS of [Co(II)-dmbpy] in aqueous dilute (0.3 mM) solution during electrochemical CO$_2$ reduction and discussed Co K-edge X-ray absorption near edge structure (XANES) spectra by combination with density functional theory (DFT) calculations.[4] However, *operando* XAS measurement for the molecular metal complexes under light-irradiated suspension mixed with semiconductor particles is challenging to establish a measurement setup, including reactor design, due to the complexity of the system. In this study, we succeeded in directly observing dilute Co complex redox mediators in an aqueous solution suspended with photocatalysts using *operando* XAS. We first attempted to measure the Co K-edge XANES spectra of divalent and trivalent [Co-dmbpy] complexes alone ([Co(II)-dmbpy] and [Co(III)-dmbpy]) in a CO$_2$-saturated 10 mM NaHCO$_3$ aqueous solution, which is the same as the solution used in the photocatalytic reaction described below. To prevent synchrotron radiation from reducing Co(III) to Co(II), standard XANES spectra of the Co(II) and Co(III) complexes were successfully obtained by stirring a large (100 mL) 0.3 mM solution during measurement. This large-volume approach effectively mitigates beam-induced damage in suspension-based systems.[7] In Co K-edge XANES spectra, a shift of about 2.3 eV between the Co(II) and Co(III) peak positions was observed, suggesting that the method is applicable to observe the behavior of Co species during photocatalysis, with the signal-to-noise ratio (SNR) calculated as 101 (Fig. S1 and S2). Subsequently, Co K-edge *operando* XAS measurements were conducted on a visible-light-driven Z-scheme

CO$_2$ reduction system in an aqueous suspension containing [Co(II)-dmbpy], BiVO$_4$, and CGZS. The semiconductors and Co complexes used in this *operando* study were confirmed to exhibit photo-catalytic activity comparable to previously reported[3] levels in a visible-light-driven Z-scheme reaction using a CO$_2$ flow reactor and a batch-type reactor (Fig. S3a, b and Table S1). *Operando* XAS measurements in the Z-scheme reaction were performed using a Pyrex cell with a polyimide window as follows (Fig. 1(b)). Under continuous CO$_2$ flow, a CO$_2$-saturated 10 mM NaHCO$_3$ aqueous solution containing the divalent [Co(II)-dmbpy] complex was stirred, followed by the addition of two photocatalysts. The resulting suspension was kept under dark conditions with stirring for 1 h. Subsequently, visible light (λ > 420 nm) was irradiated from the side of the reaction cell while stirring was maintained. *Operando* Co K-edge XAS analyses were performed using a fluorescence yield mode, with each measurement period set at about 10 min. The light energy density for the *operando*-XAS was set identical to that of photocatalytic CO$_2$ reduction reported (see experimental section in SI). Here, most of the Co K-edge XANES spectra can be discussed as that of the electron mediator, since 98% of the [Co-dmbpy] contributes as a redox-shuttle electron mediator in the present system as (Co(II)/Co(III)).[3]

Fig. 1(c) shows representative Co K-edge XANES spectra obtained over time in the Z-scheme system in divalent [Co(II)-dmbpy] aqueous solution. The changes in the XANES spectra at detailed time steps under dark and irradiation conditions are shown in Fig. S4 and S5, respectively. To obtain deeper insight into the behavior of the Co species observed in the XANES spectra, the results are summarized in Fig. 2, which presents the time course of the Co K-edge XANES edge energies (E_{edge}) during the Z-scheme CO$_2$ reduction using [Co(II)-dmbpy] (closed blue circles). Here, E_{edge} is defined as the energy at a normalized absorption of 0.5, corresponding to the 0.5 position on the vertical axis in Fig. 1(c), as previously described.[8] The Co(II) complex exhibited an edge energy (E_{edge}) of 7716.6 eV. Upon addition of CGZS and BiVO$_4$ under dark conditions, the edge energy gradually increased (indicative of oxidation) by up to +0.7 eV, and became relatively stable after 40 min. The *ex situ* UV-Vis spectrum of the solution sampled after 1 h in the dark,
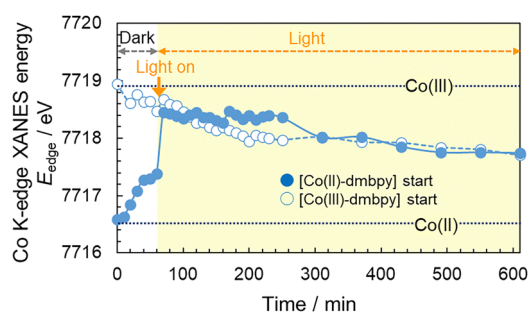

Fig. 2 Time course of the edge energies of the Co K-edge *operando* XANES (E_{edge}) during the Z-scheme CO$_2$ reduction reaction using [Co(II)-dmbpy] (closed blue circle) and [Co(III)-dmbpy] (open blue circle). E_{edge} values were defined as the energies at a normalized absorption of 0.5, as shown in the Fig. 1(c). The horizontal axis represents the total elapsed time in dark and light conditions.

following removal of the solid photocatalysts, and 12-fold dilution of the filtrate, showed a decrease in the Co(II)-related peak and the emergence of a new peak corresponding to Co(III) (Fig. 1(d), blue line). This is consistent with the *operando* XANES results. The presence of Co(III) species suggests that even in the dark, [Co(II)-dmbpy] was oxidized to Co(III) through electron transfer to the electron-deficient CGZS. These aspects will be discussed in detail later.

Upon irradiation, the energy value shifted steeply by about +1.0 eV, probably due to electron donation to CGZS. Then gradually shifted back toward lower energy and stabilized after 6 h of light irradiation (corresponding to 420 min, including 1 h of darkness, in Fig. 2). The final photon absorption edge energy (E_{edge}) after 9 h of light irradiation reached 7717.7 eV, which lies approximately midway between the energies of Co(II) and Co(III). From the two-component spectra of [Co(II)-dmbpy] and [Co(III)-dmbpy], Co(II) and Co(III) species were quantified to be 53% and 47%, respectively (see Experimental section in SI), indicating a near-perfect redox-buffered Co(II)/Co(III) mediator that maintains a well-balanced redox equilibrium during continuous photocatalytic CO_2 reduction. As shown in the UV-Vis spectra (Fig. 1(d)), the Co(III) component increased after 170 min of irradiation but slightly decreased after 550 min, at which point spectral deconvolution estimated Co(II) and Co(III) at 40% and 60%, respectively. The proportion of Co(III) in UV-Vis analysis was 13% higher than that obtained from direct XAS measurements because the sample preparation of dilute solutions and measurement being conducted in air as previously described (Fig. S6). These results indicate that, although the overall UV–Vis trend was consistent with the XANES results, *operando* XAS provided more precise real-time insights into Co valence changes. It is also suggested that electron transfer between BiVO$_4$ and CGZS occurs *via* the redox cycle of the Co complex, maintaining the appropriate valence of Co(II) and Co(III) in the photocatalytic reaction. These results demonstrate that *operando* XAS can monitor the *in situ* and real-time evolution of Co complex oxidation states, thereby clarifying the role of redox shuttle mediators in photocatalytic reactions. For comparison, *operando* XAS measurements were conducted using a Z-scheme system with [Co(III)-dmbpy] under the same procedure as [Co(II)-dmbpy] (blue open circles in Fig. 2). Unlike [Co(II)-dmbpy], no distinct shift to higher energy was observed upon light irradiation, and the E_{edge} before and after irradiation remained nearly identical. Instead, a gradual shift to lower energy occurred, stabilizing around 250 min (190 min of irradiation). At 610 min (550 min of irradiation), the E_{edge} reached 7717.7 eV, nearly the same as when starting from Co(II). These results suggest that, under stable conditions in this Z-scheme system, the Co(II)/Co(III) ratios in solution at the equilibrium are determined by the balance with the semiconductors added, regardless of the initial valence state of the Co complex.

To evaluate the effect of each photocatalyst (BiVO$_4$ or CGZS) on the Co complex mediator, Fig. 3 shows the time-dependent change of the Co K-edge E_{edge} during the initial dark and light processes (up to 4 h) for the two half-reactions using [Co(II)-dmbpy], together with results from the Z-scheme system
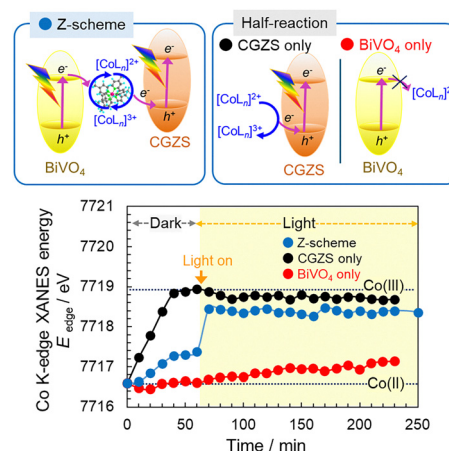

Fig. 3 Time course of the edge energies of Co K-edge *operando* XANES (E_{edge}) during the Z-scheme (blue) and half-reactions (CGZS only ⟨black⟩ or BiVO$_4$ only ⟨red⟩) in CO_2-bubbled aqueous 0.01 M NaHCO$_3$ solution containing [Co(II)-dmbpy]. The E_{edges} were defined as the energies at a normalized absorption of 0.5.

(blue circle). The Co complex behavior depends strongly on both light and the semiconductor employed. In the CGZS-only half-reaction (closed black circle), CO production was significantly reduced compared with the Z-scheme, while H$_2$ was predominantly produced over CO (Fig. S3c and S7). XAS revealed that adding CGZS to [Co(II)-dmbpy] solution in the dark caused a pronounced ∼2.33 eV E_{edge} shift to higher energy, consistent with oxidation to Co(III) (Fig. 3, black circle; Fig. S8), likely due to gradual electron donation to CGZS. Even after visible-light irradiation for 170 min (230 min total on the Fig. 3 *x*-axis), only a minor shift to lower energy was observed, and the Co species remained mainly in the Co(III) state, suggesting that back electron transfer from CGZS is not dominant in this half-reaction.

In the BiVO$_4$-only half-reaction (closed red circle), BiVO$_4$ can oxidize water under visible light, but its conduction band electrons lack sufficient energy to reduce CO$_2$ or protons, and thus no CO or H$_2$ was produced even in the presence of [Co(II)-dmbpy].[3] As shown in Fig. 3 (red circle), the E_{edge} of 7716.6 eV of [Co(II)-dmbpy] remained unchanged for 0–60 min in the dark after addition of BiVO$_4$, indicating that cobalt remained mainly in the Co(II) state. The behavior contrasts sharply with that observed in CGZS-only half-reaction, highlighting that the dark-state behavior of [Co(II)-dmbpy] strongly depends on the semiconductor photocatalyst. Following the dark-state analysis with BiVO$_4$, visible light ($\lambda > 420$ nm) was applied, and Co K-edge XANES spectra were monitored for 170 min (Fig. S9). Irradiation caused a gradual, slight shift of the edge to higher energy, and after 170 min (230 min total on the Fig. 3 *x*-axis), the distribution of Co(II) and Co(III) were estimated to be 75% and 25%, respectively. This slow oxidation likely reflects BiVO$_4$-mediated processes, partial Co(II) oxidation, or structural changes of [Co-dmbpy]. These behaviors under dark and light conditions differ markedly from those observed with CGZS-only.

The Co K-edge spectral behavior of [Co(II)-dmbpy] differs markedly among the two half-reactions and the Z-scheme. In the CGZS half-reaction, [Co(II)-dmbpy] donates an electron to

electron-accepting p-type CGZS in darkness to form fully Co(III), unlike in the BiVO$_4$ half-reaction. Without an electron donation from BiVO$_4$, Co(III) accumulates in solution, explaining the very low CO production, as previously reported[3] and as shown in Fig. S2c, since the reduction cycle cannot proceed except through self-corrosion of CGZS. In the Z-scheme system (closed blue circle) in darkness, [Co-dmbpy] exhibits suppressed electron transfer to CGZS, yielding a fairly-balanced Co(II)/Co(III) ratio of Co(II) = 56%. Upon light irradiation, further electron transfer to CGZS occurs, producing a continuous Co(III)-dominant state. This suggests that photoexcited CGZS requires more electrons at this Co(III)-dominant stage in the Z-schematic operation, but the electron supply from BiVO$_4$ is insufficient. Therefore, the results might indicate that H$_2$O oxidation at BiVO$_4$ is the rate-limiting step during this induction time region of the Z-schematic CO$_2$ reduction (Fig. S3b). After the induction period, approximately equal amounts of Co(II) and Co(III) are present in the solution. In the Z-schematic hydrogen generation by water splitting using Fe^{3+}/Fe^{2+} electron mediator and rutile TiO$_2$, TiO$_2$ particles preferentially adsorb Fe^{3+} ions. Indeed, when both Fe^{3+} and Fe^{2+} are present, only Fe^{3+} ions adsorb, leading to O$_2$ generation.[9] A similar selective adsorption of the molecular [Co-dmbpy] mediator at different oxidation states occurs on the respective semiconductor surfaces. Previous analyses of the photocatalysts and the solution after irradiation confirmed that more than 98% of the [Co-dmbpy] remains unadsorbed on the semiconductor photocatalyst.[3] This strongly suggests that [Co-dmbpy] functions as a redox shuttle, cycling between Co(II) and Co(III), and mediates electron transfer between CGZS and BiVO$_4$ in the Z-scheme CO$_2$ reduction.

This paper discusses the direct observation of the Co complex electron mediators by *operando* XAS. However, in the future, when a more sensitive detection setup for this dilute Co complex is realized, extended X-ray absorption fine structure (EXAFS) will enable a more detailed understanding. This *operando* XAS approach applies to different semiconductor/metal-complex hybrid photocatalyst suspension systems composed of particulate oxide, sulfide, or selenide semiconductors combined with metal complexes or metal cations, as the electron mediator in the Z-scheme and sacrificial electron donors for CO$_2$ reduction.[2,10] The *operando* XAS in aqueous solution could also contribute to systems of hydrogen generation by water splitting using as electron mediators consisting of metal complexes[11] and metal ions.[9,12]

In summary, *operando* XAS enabled direct, real-time observation of the redox behavior of the cobalt complex [Co(II)-dmbpy], which acts as a redox-shuttle electron mediator in Z-scheme photocatalytic CO$_2$ reduction with BiVO$_4$ and CGZS. The behavior of [Co(II)-dmbpy] underscores the critical dependence of its redox state on the presence of both semiconductors and visible light, and highlight its unique functionality in maintaining electron transfer during the Z-schematic reaction.

Conflicts of interest

There are no conflicts to declare.

Data availability

The data supporting this article (CO$_2$ reduction, *etc.*) are included in the supplementary information (SI). Supplementary information is available. See DOI: https://doi.org/10.1039/d5cc05617a.

Notes and references

1 (*a*) W. Zhang, A. R. Mohamed and W. J. Ong, *Angew. Chem., Int. Ed.*, 2020, **59**, 22894–22915; (*b*) S. Yoshino, T. Takayama, Y. Yamaguchi, A. Iwase and A. Kudo, *Acc. Chem. Res.*, 2022, **55**, 966–977.
2 T. M. Suzuki, S. Yoshino, T. Takayama, A. Iwase, A. Kudo and T. Morikawa, *Chem. Commun.*, 2018, **54**, 10199–10202.
3 T. M. Suzuki, S. Yoshino, K. Sekizawa, Y. Yamaguchi, A. Kudo and T. Morikawa, *Appl. Catal., B*, 2022, **316**, 121600.
4 T. M. Suzuki, K. Nagatsuka, T. Nonaka, Y. Yamaguchi, N. Sakamoto, T. Uyama, K. Sekizawa, A. Kudo and T. Morikawa, *Chem. Commun.*, 2023, **59**, 12318–12321.
5 H. Issa Hamoud, L. Wolski, I. Pankin, M. A. Bañares and M. El-Roz, *Top. Curr. Chem.*, 2022, **380**, 37.
6 (*a*) H. Lyu, T. Hisatomi, Y. Goto, M. Yoshida, T. Higashi, M. Katayama, T. Takata, T. Minegishi, H. Nishiyama, T. Yamada, Y. Sakata, K. Asakura and K. Domen, *Chem. Sci.*, 2019, **10**, 3196–3201; (*b*) L. Piccolo, P. Afanasiev, F. Morfin, T. Len, C. Dessal, J. L. Rousset, M. Aouine, F. Bourgain, A. Aguilar-Tapia, O. Proux, Y. Chen, L. Soler and J. Llorca, *ACS Catal.*, 2020, **10**, 12696–12705; (*c*) Z. Wang, R. Toyoshima, M. Yoshida, K. Mase and H. Kondoh, *J. Phys. Chem. C*, 2024, **128**, 9193–9201.
7 K. I. Yamanaka, K. Sato, S. Sato, S. Nozawa, S. H. Lee, R. Fukaya, H. Fukuzawa, D. H. Y. You, S. Saito, T. Takanashi, T. Katayama, T. Togashi, T. Nonaka, K. Dohmae, S. I. Adachi, K. Ueda, M. Yabashi, T. Morikawa and R. Asahi, *J. Photochem. Photobiol., A*, 2023, **435**, 114267.
8 T. Uyama, Y. Noda, T. M. Suzuki, K. Sekizawa, N. Sakamoto, T. Nonaka and T. Morikawa, *Chem. Mater.*, 2025, **37**, 3327–3342.
9 Y. Wang, H. Suzuki, J. Xie, O. Tomita, D. J. Martin, M. Higashi, D. Kong, R. Abe and J. Tang, *Chem. Rev.*, 2018, **118**, 5201–5241.
10 (*a*) M. F. Kuehnel, C. D. Sahm, G. Neri, J. R. Lee, K. L. Orchard, A. J. Cowan and E. Reisner, *Chem. Sci.*, 2018, **9**, 2501–2509; (*b*) K. Maeda, *Adv. Mater.*, 2019, **31**, 1808205; (*c*) A. Nakada, H. Kumagai, M. Robert, O. Ishitani and K. Maeda, *Acc. Mater. Res.*, 2021, **2**, 458–470; (*d*) T. Morikawa, S. Sato, K. Sekizawa, T. M. Suzuki and T. Arai, *Acc. Chem. Res.*, 2022, **55**, 933–943.
11 (*a*) Y. Sasaki, H. Kato and A. Kudo, *J. Am. Chem. Soc.*, 2013, **135**, 5441–5449; (*b*) T. Kato, Y. Hakari, S. Ikeda, Q. Jia, A. Iwase and A. Kudo, *J. Phys. Chem. Lett.*, 2015, **6**, 1042–1047.
12 (*a*) R. Abe, K. Sayama, K. Domen and H. Arakawa, *Chem. Phys. Lett.*, 2001, **344**, 339–344; (*b*) Y. Bai, K. Nakagawa, A. J. Cowan, C. M. Aitchison, Y. Yamaguchi, M. A. Zwijnenburg, A. Kudo, R. S. Sprick and A. I. Cooper, *J. Mater. Chem. A*, 2020, **8**, 16283–16290; (*c*) Y. Miseki and K. Sayama, *Adv. Energy Mater.*, 2018, **9**, 1801294; (*d*) D. M. Fabian, S. Hu, N. Singh, F. A. Houle, T. Hisatomi, K. Domen, F. E. Osterloh and S. Ardo, *Energy Environ. Sci.*, 2015, **8**, 2825–2850.